Available online at www.sciencedirect.com
SCIENCE DIRECT®
International Journal of Mass Spectrometry 232 (2004) 1–7
International Journal of Mass Spectrometry
www.elsevier.com/locate/ijms

Surface impact induced fragmentation and charging of neat and mixed clusters of SO_2 and H_2O

V.V. Gridin [b], C.R. Gebhardt [a,*], A. Tomsic [a], I. Schechter [b], H. Schröder [a], K.L. Kompa [a]

[a] *Max-Planck-Institut für Quantenoptik, Hans-Kopfermann-Straße 1, D-85748 Garching, Germany*
[b] *Department of Chemistry, Technion-Israel Institute of Technology, Haifa 32000, Israel*

Received 16 September 2003; accepted 28 October 2003

Abstract

Cluster impact induced charge separation was studied with neat and mixed clusters of SO_2 and H_2O impinging at hyperthermal velocities on a SiO_x target held at different temperatures. At 750 K, impact of SO_2 clusters produces positively and negatively charged cluster fragments of the form $[(SO_2)_n - K, Na]^+$ and $[(SO_2)_m - SO_2]^-$ which is explained in terms of the known cluster-impact induced pickup of alkali surface adsorbates. The high sensitivity of this channel promises applications for the analysis of alkali surface contaminations. The dominant fragments observed during the impact of binary SO_2/H_2O clusters at the same target temperature were $[(H_2O)_n - H]^+$ and $[(SO_2)_p (H_2O)_q - HSO_3]^-$, which indicates an intracluster proton transfer reaction. Similar fragments were also detected as minor spectral progressions during the surface impact of neat SO_2 clusters at a target temperature of 380 K. This is interpreted in terms of an impact-induced pickup of water surface adsorbates into the neat sulfur dioxide cluster during the surface collision. Upon impact of neat water clusters, fragment ions of the form $[(H_2O)_n - H]^+$ and $[(H_2O)_q - OH]^-$ are observed, which can be explained in terms of the autoprotolysis reaction in bulk water.

PACS: 36.40.In; 82.30.Fi; 82.80.Ms

Keywords: Molecular clusters; Charge transfer; Cluster impact

1. Introduction

Molecular clusters are readily formed through condensation in supersonic expansions. When seeded in H_2 or He as buffer gas, they typically reach hyperthermal velocities corresponding to an energy per molecule of up to ≈1 eV. This energy is sufficient to fragment the cluster during surface impact by breaking the relatively weak intermolecular bonds, but it is insufficient to break the intramolecular chemical bonds. However, the observed formation of positive and negative cluster fragments upon cluster impact, termed the clusterelectric effect (CEE), indicates that low barrier charge transfer reactions can still proceed, either in the intact cluster or during the short time of surface contact which is on the order of a few picoseconds. Examples are the spontaneous ionization of alkali atoms in polar solvents [1,2] as well as the self-ionization of neat nitric acid [3]. By using a combination of mass spectrometry and cluster surface collisions of neutral molecular clusters, these charge transfer processes can be studied under bulk like densities. From the respective mass spectra also information concerning the microsolvation of the respective charge carriers as well as solvent structures of special stability, so called magic numbers, can be obtained. Clearly, our approach is directed towards a mass spectrometry of electrolytic solutions [4], but one has to be cautious. Small aggregates have properties that often differ significantly from those of the bulk and typically display behavior that is not fully characterized as being due to a solid, liquid or gas [5]. This is mainly caused by the large fraction of surface molecules [6]. For instance, the diffusion coefficient, the electrical conductivity, the H-bond arrangement and the viscosity of the water ice surface is not the same as in the bulk [7]. Also proton transfer reactions can be influenced by the finite size of the cluster [8]. Keeping this in mind, nevertheless valuable insight into solution phase charge transfer reactions can be obtained via cluster surface collisions.

* Corresponding author. Tel.: +49-89-32905230; fax: +49-89-32905200.
E-mail address: Christoph.Gebhardt@mpq.mpg.de (C.R. Gebhardt).

1387-3806/$ – see front matter © 2003 Elsevier B.V. All rights reserved.
doi:10.1016/j.ijms.2003.10.003

Using the system water/sulfur dioxide, we investigate binary clusters for which normal solution phase chemistry predicts the occurrence of spontaneous charge transfer reactions. The proton transfer reaction observed in bulk solutions of SO_2 in H_2O can formally be written as

$$SO_{2,aq} + H_2O \rightleftharpoons [HSO_3]^- + H_3O^+. \quad (1)$$

The chemistry of aqueous solutions of sulfur dioxide is however more complicated than might appear from Eq. (1). For the bisulfite ion $[HSO_3]^-$, actually two different isomeric forms have been characterized, namely H–SO_3^- and H–OSO_2^- [9]. Given the close values for the proton affinity of water with 7.22 eV and sulfur dioxide with 7.01 eV, the exclusive formation of H_3O^+ is also surprising and indicates the importance of the ion microsolvation on the reaction. The affinity of the OH^- to sulfur dioxide, however, can be rationalized with the considerably higher bond strength in the OH–SO_2^- bisulfite of 2.68 eV as compared to 1.15 eV of the OH–H_2O^- bond. The molecular form of sulfurous acid H_2SO_3 has not been observed experimentally as a stable compound. This is in accordance with recent quantum chemical calculations that found H_2SO_3 to be thermodynamically unstable under standard conditions [10,11]. Until now, corresponding calculations for the ionic reaction path are not available. Due to its atmospheric relevance [12,13], the system of water and sulfur dioxide has been studied experimentally via optical spectroscopy [14–16], in protonated binary clusters following laser ionization [17], as well as in ion clustering experiments [18–20]. Here we investigate the system using our cluster impact mass spectrometry technique which starts from all neutral clusters. For neat sulfur dioxide clusters, we present results on electron transfer reactions induced by pickup of alkali surface adsorbates. With additional water surface adsorbates offered to the incident SO_2 clusters, a proton transfer channel, forming the ionic species in Eq. (1), is clearly observed. We then move on to binary SO_2/H_2O clusters in which the same reaction is directly observed following cluster fragmentation. Finally, we show that also in neat water clusters a proton transfer reaction can be observed which can be explained in terms of the autoprotolysis reaction of water.

2. Experimental

Fig. 1 gives a schematic view of the molecular cluster beam apparatus. Both chambers are pumped by a combination of turbomolecular pumps with membrane pumps to reduce the hydrocarbon contamination. The main components include: a temperature controlled high pressure gas handling system, a pulsed nozzle to produce a supersonic free jet expansion ($d = 0.5$ mm, typical pulse width 300 μs), a skimmer ($d = 1.5$ mm) for beam clipping and gas load reduction in the second chamber, a heatable collision target, and a home-designed pulsed Wiley-MacLaren type time-of-flight mass spectrometer. The nozzle skimmer distance is 7 cm

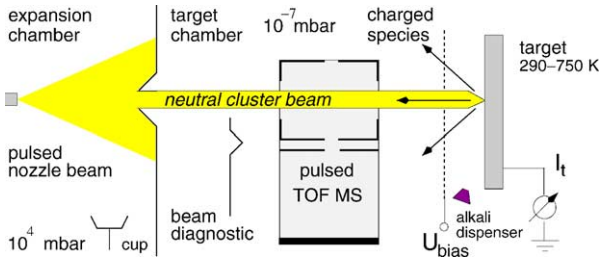

Fig. 1. Experimental setup. The pressures are given with the molecular beam on.

and the nozzle target distance is 30 cm. A bias grid (≈ 10 lines/in.) placed 10 mm in front of the target allows for measuring total charge yields per pulse by pushing one ion polarity against the target for neutralization. It also serves to transfer fragment ions into the extraction volume of the mass spectrometer. An oxalate based alkali atom dispenser is optionally used for surface dosing. When applying positive or negative high voltage pulses, ions from the center of the extraction volume are accelerated onto the grounded MCP detector, where they impinge at an energy of 5.2 kV. Where indicated, the mass dependent detector sensitivity has been corrected following [21]. The collision target consisted of a commercial silicon wafer with its natural oxide layer, that was placed into the chamber, pumped for several hours and then heated to 750 K for several hours. While hydrocarbon contaminations were detected in mass spectra taken at room temperature, their amount reduced below our detection limit when the surface temperature was raised to 380 K. The cluster size distribution of the incident beam is measured with the retarding field technique [22] following ionization of the beam with 30-eV electrons. The $N^{2/3}$ dependence of the geometrical ionization cross section for the clusters has been taken into account in the cluster size determination. Assuming ideal conditions, the beam velocity has been calculated from the expansion parameters [23]. In order to control the stability of the nozzle and to assess the overall performance of a particular cluster species, chamber I is equipped with a charged particle probe at a bias voltage of ±30 V, to collect charges generated at the skimmer rim.

3. Alkali induced CEE

Fig. 2 represents typical charged fragment spectra from our standard reference experiment, in which a SO_2 cluster beam is scattered off an untreated SiO_x wafer surface held at a temperature of about 750 K. The cluster size distribution in the incident beam is well represented by a log-normal distribution $f(N)$,

$$f(N) = \exp\frac{(-(\ln(N) - m)^2/(2s^2))}{(\sqrt{2\pi}Ns)} \quad (2)$$

with the parameters $m = 6.0$ and $s = 0.95$, and thus by a mean cluster size of $\langle N\rangle = \exp(m + 0.5s^2) = 0.63 \times 10^3$.

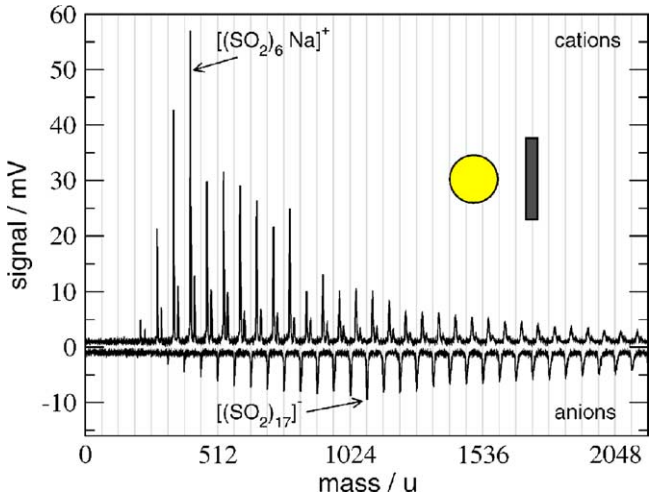

Fig. 2. Mass spectra of the positively and negatively charged cluster ions generated by the impact of pure SO_2 clusters on the target heated to 750 K.

The beam velocity of 1.3 km s^{-1} corresponds to a kinetic energy of 0.52 eV per particle, which is a factor of two larger than the standard heat of vaporization for SO_2. The resultant fragments are of the form $[(SO_2)_n - Na, K]^+$ and $[(SO_2)_n - SO_2]^-$. As has been discussed previously [1], the observed spectra can be explained in terms of pickup of ubiquitous alkali surface adsorbates during the cluster impact. Inside the polar molecule cluster, the alkali atom ionizes spontaneously [24] forming an electron-cation pair which is subsequently mechanically separated by the collision induced cluster fragmentation.

4. CEE sensitivity

Typical alkali coverages on silicon wafers are on the order of 10^9–10^{10} cm^{-2}. The strong signals and the good signal to noise ratio of the mass spectra in Fig. 2 reveal that this amount of coverage is easily detected with our method and indicate its analytical potential regarding alkali contaminations on surfaces. A typical monomer flux per pulse onto the target is 10^{13} cm^{-2} in our experiments. These monomers are condensed into clusters. Using the cluster size distribution from above, this means that 10^{10} cm^{-2} clusters per pulse are hitting the target. With a mean cluster area of $\langle N\rangle^{2/3} = 73$ times the cross section of a sulfur dioxide molecule of $\pi r^2_{SO_2} \approx 10^{-15}$ cm^2, this means that 10^{-3} of the exposed area of 0.5 cm^2 is sampled. Assuming an uptake probability of one we expect between 10^6 and 10^7 charge carriers for the above values for alkali contamination on silicon wafers. This estimation is confirmed by absolute yield measurements as described in the experimental section. Since even single charges can technically be measured, the present method promises an extremely high sensitivity for adsorbed alkali atoms. A conservative estimate brings the detection limit to below 10^5 cm^{-2}, which is orders of magnitude better than any other known technique [25]. Furthermore, only the analyte atoms are removed, the substrate itself remains unaffected because the energy per cluster particle is quite low (<1 eV).

5. Magic numbers

Fig. 3 gives peak integrals for the individual progressions in Fig. 2. Dominant peaks, marked by stars, indicate cluster configurations of enhanced stability quite independent of how they are formed. The solvation of Na^+ with SO_2 clearly shows enhanced stabilities for $N = 6, 12$. Contrary, a fourfold coordination in the gas phase [26,27] and a rather smooth envelope in the range up to 17 water molecules [28,29], as well as a six-fold coordination in the condensed phase is observed or predicted in the case of hydration of sodium ions. The less structured solvation shell around the potassium core ion is in accordance with similar findings in water [30]. The late onset of magic numbers for the SO_2^- core ion was previously observed in [31]. It has been shown in electrospray mass spectrometry [32], that the structure of an ion pair in an electrolytic solution can be discussed on the basis of the mass spectrometric analysis of the solvation shell of the ions extracted from the liquid. However, the observed microstructures, especially the observed magic numbers, are generally quite different from the situation in the bulk solvent, due to the large fraction of surface molecules [6]. Consequently, the observed intensity variations in the mass spectra reflect the ion–solvent interaction much stronger than the solvent–solvent interaction, which is more important in bulk solutions.

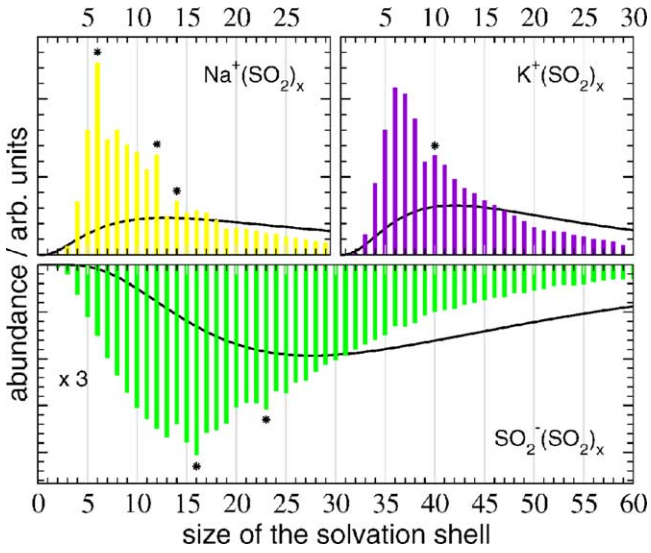

Fig. 3. Normalized peak height distributions for the various core ion progressions observed in Fig. 2. Bar graphs give the integrated peak areas from the spectra as measured. Solid lines give log-normal envelopes, fitted to the peak height distributions after correcting for the mass-dependent detector sensitivity [21]. Stars mark structures of enhanced stability.

6. Fragment size distribution

The fragment size distribution in Fig. 3 seems to be unusual because it does not exhibit the universal power law dependence [33]. The observed cut off towards small solvent shells can be rationalized in terms of the higher binding energies of the very small ionic fragments e.g., $[SO_2 - SO_2]^- \approx 1\,eV$ $[(SO_2)_2 - SO_2]^- \approx 0.35\,eV$ [31] which exceed the binding energy between the neutral cluster constituents. Also the long tail of the observed size distributions for cations and even more for anions is remarkable. After correction for the mass dependent detector sensitivity (solid line in Fig. 3), a more or less constant yield between $[(SO_2)_{20}]^-$ and $[(SO_2)_{40}]^-$ is observed. According to [34] this would indicate that we are not in the fragmentation regime where shattering to small pieces occurs but rather in the damage regime with the survival of larger entities. Inspection of the cation and anion envelopes in Fig. 3 reveals that the cations are considerably smaller than the anions. This is quite generally observed when pickup of alkalis is the origin of the charge creation. We propose a simple explanation in terms of the different mobility of alkali ions and electrons. On the time scale of the surface impact, which lasts only a few picoseconds, the alkali ion cannot diffuse into the cluster since a diffusive motion takes typically on the order of some 10 ps over only one intermolecular distance. Therefore, only molecules from the contact area are available for the charged fragment formation. Contrarily, the highly mobile electrons can accommodate at the most appropriate site within the entire cluster. In accordance with this, the envelopes become comparable when the initial charge transfer does not involve free electrons, that is the case e.g. for the self-ionization in HNO_3 clusters [3].

7. Water covered surface

The mass spectra shown in Fig. 2 have been taken at a relatively high surface temperature (750 K) to avoid interference with molecular adsorbates. At reduced temperatures molecules from the background gas (10^{-7} mbar, mostly water) can accumulate on the surface or surface adsorbates having their origin in target preparation procedures are not sufficiently removed. The presence of adsorbates at surfaces like water or hydrocarbons under high vacuum conditions and at low to moderate surface temperatures is an established fact. It has been employed advantageously in a variety of experiments e.g., studying the interaction of molecular or cluster ions with the adsorbed species in surface collisions [35,36].

A typical example spectrum obtained under such conditions, again for SO_2 clusters ($\langle N\rangle = 0.63 \times 10^3$, $v_i = 1.3\,km\,s^{-1}$, SiO_x at 380 K), is given in Fig. 4. Overall, less charges are observed and the spectra have become notably more complicated. The assignment reveals that new spectral features are superimposed on the alkali based progressions. For the cations we find an additional $[(SO_2)_n - (H_2O)_4 - H]^+$

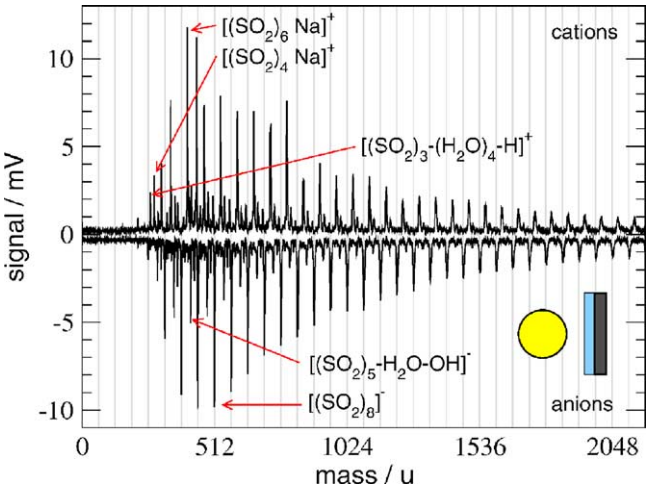

Fig. 4. Mass spectra of the positively and negatively charged cluster ions generated by the impact of pure SO_2 clusters on a surface containing water adsorbates (target temperature 380 K).

and $[(SO_2)_n - (u = 32) - H_2O) - H]^+$ progressions ($n \geq 3$) wherein $u = 32$ most probably is due to a methanol molecule from the background gas. Progressions with an increasing water content similar to the sulfur dioxide case are not observed. The dominant peaks in the anion spectrum of Fig. 4 are still $[(SO_2)_n - SO_2]^-$ from the $(SO_2)_{cluster} + (Na, K)_{ads} \rightarrow [(SO_2)_m - (Na, K)]^+ + [(SO_2)_n - SO_2]^-$ reaction but also new progressions such as $[(SO_2)_{1+m} - (H_2O)_n - CH_3OH - OH]^-$ ($m \geq 0, 0 < n <\approx 10$) have appeared. The strongest members are $[(SO_2)_{1+p} - (H_2O)_1 - OH]^-$ fragments and $[(SO_2)_{1+p} - CH_3OH - OH]^-$, the $[(SO_2)_{1+p} - (H_2O)_2 - OH]^-$ fragments seem to be missing. Obviously, water is the crucial agent to promote the creation of the additional charge pairs. At 380 K only chemisorbed water can be expected and because at least five water molecules are necessary to yield our smallest entity $(SO_2)_p(4H_2O + H^+ + OH^-)$ we conclude that water islands play the key role. Furthermore, we have some evidence that when the water channel increases, the alkali channel decreases or even disappears. This suggests that water islands preferentially accommodate on alkali adsorbates and furthermore that pickup of alkalis is hindered by the water overlayer. Alkali coadsorbed water has been reported for a number of well studied systems [37]. The clue seems to be that the pristine SiO_x surface is hydrophobic, whereas the local electric field in the immediate vicinity of adsorbed alkali metal species will attract water molecules [38]. Moreover, ion pair or zwitterionic structures are conceivable [39]. Unfortunately, conventional characterization of the water coverage seems to be challenging owing to the low concentration of perhaps less than 10^{-4} monolayers. The ease with which such low coverages of water surface adsorbates are detected using neutral cluster impact again stresses the surface analytical potential of this method. It represents a variant of the established chemical sputtering method [40] in which surface adsorbates are transferred into the gas

phase by low energy ion impact and ionized concomitantly by charge transfer processes. In retrospect, the first experiment of neat SO_2 cluster impact on the target surface at 750 K can be viewed as a surface characterization, giving an upper limit of 10^{-6} monolayers for the water coverage.

We have two possibilities in mind to rationalize the observed ionic water dissociation upon SO_2 cluster impact. Water might be available in a sort of preionized precursor state that is picked up by the cluster and subsequently separated by cluster fragmentation or we are facing a simple water uptake followed by fast proton transfer. Uptake experiments of SO_2 (g) by aqueous surfaces have shown the facile formation of a $HSO_3^- - H^+$ surface complex in equilibrium with the gas phase SO_2 [14]. Indeed, if this reaction would be responsible it must be very fast because the available time window between contact and fragmentation is less than a few picoseconds (cluster diameter/impact velocity v_i) [41]. Charge pairs formed on a longer time scale, e.g., in the cluster fragments, would not get separated since stabilization of the fragments by evaporation of neutral monomers is the dominant channel due to their smaller binding energy. Consequently, such ion pairs cannot be detected by our mass spectrometric method.

8. Mixed clusters

The spectra in Fig. 5 represent the seemingly simpler case when binary SO_2/H_2O clusters interact with a hot (750 K) SiO_x surface, where no influence of water adsorbates was detected for cluster impact of neat SO_2 clusters. We might regard this as a direct mass spectrometric inspection of a classical acid base reaction [3]. The clusters were produced by bubbling a 10 bar 14:1 He/SO_2 mixture through water at room temperature. Understanding the morphology and the exact composition of two-component clusters is a matter of active research [42–44]. In the present case, due to their lower vapor pressure, the water molecules in the beam condense first. Since the sticking coefficient of SO_2 on water surfaces is only 0.1 [14] and since above 120 K a large part of SO_2 diluted in water ice escapes [16], we expect the formed clusters to consist predominantly of water. As shown in Fig. 5, intense cations and anion spectra can be recorded for the impinging SO_2/H_2O clusters. The overwhelming majority of cations are merely protonated water molecules $[(H_2O)_n - H]^+$ with only a few percent of attached SO_2. A prominent feature in the cation spectrum is the enhanced stability of $[(H_2O)_{21} - H]^+$ which is commonly interpreted as a dodecahedron encapsuled hydronium ion [19] but we cannot do justice to the vast literature on this point. The anion spectrum can be described in terms of a single progression, $[(SO_2)_n - (H_2O)_m - OH]^-$, with comparable content of SO_2 and H_2O. The smallest discernible anion is $[SO_2 - OH]^-$, equivalent to the bisulfite ion $[HSO_3]^-$. This onset, however, cannot be correlated with the minimum cluster size necessary for the proton transfer to take place. The mass spectra show only the fragments of the original cluster, which in addition have undergone considerable stabilization by monomer evaporation. Anion fragments with $n \leq 5$ carry very long water sequences with some intermediate maxima, whereas for $n > 5$ only gradually decreasing sequences ($0 \leq m \leq\approx 10$) are observed. The much higher concentration of SO_2 in the solvation shells of the anions can be rationalized at least for the smaller fragments in terms of known ion clustering data [18]. Having a large quadrupole moment which is attractive towards negative ions, SO_2 substitutes water molecules in the hydration shell of OH^- [19]. On the other hand, the spectra indicate that it is energetically favorable to solvate H_3O^+ by water molecules instead of sulfur dioxide.

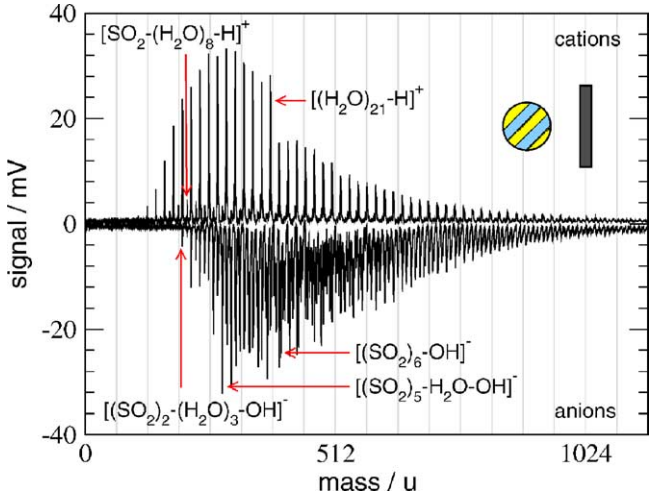

Fig. 5. Mass spectra of the positively and negatively charged cluster ions generated by the cluster surface impact of mixed H_2/SO_2 clusters. The target was held at 750 K.

Fig. 5 reveals that a proton transfer process is taking place inside the mixed cluster. Contrary to the case of the water pickup from the surface, a time window of several hundred microseconds (the flight time of the cluster to the surface) is now available for the reaction. The observed charge pair formation may occur either during cluster formation, cluster drift or during cluster impact. While the cluster spends most time on the drift towards the target, it is rather cold at this moment, with internal temperatures most likely below 10^2 K due to the efficient cooling in the carrier gas. However, thin film infrared spectroscopy between 10 and 200 K indicates that SO_2 deposited on a water ice surface or trapped in the ice bulk shows no observable reaction even after annealing [16]. This observation can be rationalized in terms of the substantial molecular rearrangement necessary to solvate the ions formed in the reaction, which is impeded by the low temperature. Yet, from NMR experiments at $-35\,^{\circ}C$ we know that the proton hopping time for ice powder is 10^{-9} s which is closer to the value in liquid water (10^{-12}) [45] than in bulk ice (10^{-4}) and it was concluded that even at $-100\,^{\circ}C$ the protons in at least the surface monolayer may move at a rate orders of magnitude faster than in bulk ice [7]. Recalling that clusters have very large surface to volume

ratios, and that depending on the expansion conditions they might have an amorphous and defect rich structure, these findings imply that a charge transfer cannot be excluded during the drift phase of the cluster. During cluster formation, the charge transfer reaction can take place via the previously mentioned HSO_3^-–H^+ surface complex. Cluster temperature at this stage is higher, due to the binding energy released into the cluster during each monomer addition. Finally, reaction may take place also during the surface impact when the SO_2/H_2O mixture experiences a solid–liquid–gas phase transition. Restriction here is mainly the short picosecond time window available to the reaction. While this is generally too fast for bimolecular reactions, electron and proton transfer processes are conceivable.

9. Water autoprotolysis

Finally, experiments have been performed with pure water clusters. Also for the neat system a proton transfer reaction is expected, namely the well known autoprotolysis reaction [46]

$$H_2O + H_2O \rightleftharpoons OH^- + H_3O^+. \quad (3)$$

Under standard condition this reaction produces about 6×10^{13} ions of each polarity per cubic centimeter in the bulk. Also in clusters spontaneous charge separation into a zwitterionic configuration has been predicted, e.g., for some isomers of dodecahedral water [47,48]. In experiments investigating the collision of water clusters with a great variety of target surfaces [49–51], water autoprotolysis was used as explanation for the observed generation of positive and negative charge carriers, although a direct mass spectrometric identification of the reaction products was not available. Fig. 6 shows mass spectra related to the charge carriers emerging in the impact of water clusters with mean size $\langle N \rangle = 2 \times 10^3$ having a velocity of $v_i = 1.7\ \mathrm{km\,s^{-1}}$ on a SiO_x surface at 690 K. Although the overall signal strength is quite low, we observe the expected $[(H_2O)_n - H]^+$ and $[(H_2O)_n - OH]^-$ features with the enhanced stabilities for $[(H_2O)_{21} - H]^+$ and $[(H_2O)_{17} - OH]^-$. As discussed above, we cannot exclude the participation of water surface adsorbates to the charge generation. A striking feature of the spectra shown in Fig. 6 as compared to the ones in Fig. 2, is the absence of strong progressions based on the pickup of alkali surface adsorbates. The same is true for Fig. 5, where the incident clusters consist also predominantly of water. By increasing the natural alkali contamination using an sodium oven source, we nevertheless could recover the expected $[(H_2O)_n - Na]^+$ progressions, which superimpose on the proton transfer progressions. Two reasons might be responsible for this seemingly lower sensitivity of water clusters towards the alkali channel as compared to SO_2 clusters. Either, as mentioned above, a water overlayer accommodating on the alkali adsorbates hinders the pickup; or, the lower overall energy available in the cluster surface collision makes the alkali desorption less probable: for equal velocities, the kinetic energy of water clusters is a factor of 3.5 lower than for sulfur dioxide clusters, due to their lower molecular weight. Under our experimental conditions the difference still is a factor of 1.9. Moreover, the stronger binding between water molecules as compared to sulfur dioxide is dissipating a larger fraction of this kinetic energy by fragment formation.

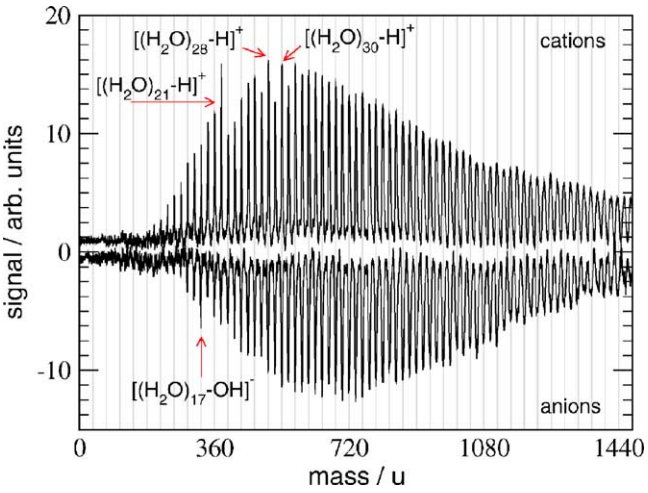

Fig. 6. Direct observation of the self-ionization in water clusters by cluster surface collisions. The target was held at 690 K.

10. Outlook

Charge transfer reactions in neat and mixed molecular clusters of sulfur dioxide and water have been investigated. Besides the known alkali induced electron transfer channel in these systems, direct mass spectrometric evidence was given for an independent proton transfer channel. In general, we have shown that cluster fragmentation at hyperthermal velocities is a simple but useful technique for mass spectrometric detection of both cations and anions, resulting from spontaneous charge transfer reactions. In a sense cluster impact fragmentation freezes dynamical fluctuations in the charge transfer processes and allows to catch a glimpse of the dynamics [52]. Because clusters can be made from all kinds of molecules and molecular mixtures also salt solutions or immiscible systems should be amenable to investigation. It should be emphasized that the charge carriers are created without externally providing the respective ionization energy via electron or laser beams. This implies a number of technical applications, e.g., for electric propulsion systems [53]. In many cases, adsorbed surface species like water and alkali metals are involved in charge pair formation and cluster fragmentation. This effect may be used for surface analysis or to transfer larger molecules e.g., of biological interest into the gas phase for mass spectrometric analysis. In particular alkali contaminants can be detected with hitherto unprecedented sensitivity.

Acknowledgements

This work was supported by the BMBF under the EEF program (02EEF137) and by the DFG within the SFB377.

References

[1] C.R. Gebhardt, H. Schröder, K.L. Kompa, Nature 400 (1999) 544.
[2] F. Eusepi, A. Tomsic, C.R. Gebhardt, Anal. Chem. 75 (2003) 5124.
[3] C.R. Gebhardt, T. Witte, K.L. Kompa, CHEMPHYSCHEM 4 (2003) 308.
[4] H. Kobara, A. Wakisaka, K. Takeuchi, T. Ibusuki, J. Phys. Chem. A 106 (2002) 4779.
[5] V. Molinero, D. Laria, R. Kapral, J. Chem. Phys. 109 (1998) 6844.
[6] J. Jortner, Z. Phys. D 24 (1992) 247.
[7] V.F. Petrenko, R.W. Whitworth, Physics of Ice, Oxford University Press, London, 1999.
[8] S. Consta, R. Kapral, J. Chem. Phys. 101 (1994) 10908.
[9] D.A. Horner, R.E. Connick, Inorg. Chem. 25 (1986) 2414.
[10] E. Bishenden, D.J. Donaldson, J. Phys. Chem. 102 (1998) 4638.
[11] A.F. Voegele, C.S. Trautermann, T. Loerting, A. Hallbrucker, E. Mayer, K.R. Liedl, Chem. Eur. J. 8 (2002) 5644.
[12] J.H. Seinfeld, Atmospheric Chemistry and Physics of Air Pollution, Wiley, New York, 1986.
[13] O. Möhler, T. Reiner, F. Arnold, J. Chem. Phys. 97 (1992) 8233.
[14] J.T. Jayne, P. Davidovits, D.R. Worsnop, M.S. Zahnisier, C.E. Kolb, J. Phys. Chem. 94 (1990) 6041.
[15] Z. Zhang, G.E. Ewing, Spectrochim. Acta Part A 58 (2002) 2105.
[16] L. Schriver-Mazzuoli, H. Chaabouni, A. Schriver, J. Mol. Struct. 644 (2003) 151.
[17] Q. Zhong, S.M. Hurley, A.W. Castleman, Int. J. Mass Spectrom. 186/187/188 (1999) 905.
[18] X. Yan, A.W. Castleman Jr., J. Phys. Chem. 95 (1991) 6182.
[19] A.W. Castleman Jr., Int. J. Mass Spectrom. Ion Processes 118/119 (1992) 167.
[20] J.R. Vacher, E.L. Luc, M. Fitaire, Int. J. Mass Spectrom. Ion Processes 135 (1994) 139.
[21] D. Twerenbold, D. Gerber, D. Gritti, Y. Gonin, A. Netuschill, F. Roessel, D. Schenker, J.-L. Vuilleumier, Proteomics 1 (2001) 66.
[22] O.F. Hagena, W. Obert, J. Chem. Phys. 56 (1972) 1793.
[23] D. R. Miller, Free jet sources, in: G. Scoles (Ed.), Atomic and Molecular Beam Methods, vol. 1, Oxford University Press, London, 1988, p. 14 (Chapter 2).
[24] I.V. Hertel, C. Hüglin, C. Nitsch, C.P. Schulz, Phys. Rev. Lett. 67 (1991) 1767.
[25] M. Yamagami, M. Nonoguchi, T. Yamada, Z. Shoji, T. Utaka, S. Nomura, K. Taniguchi, H. Wakita, S. Ikeda, X-Ray Spectrom. 28 (1999) 451.
[26] G.N. Patwari, J.M. Lisy, J. Chem. Phys. 118 (2003) 8555.
[27] M. Carrillo-Trip, H. San-Martin, I. Ortega-Blake, J. Chem. Phys. 118 (2003) 7062.
[28] F. Schulz, B. Hartke, CHEMPHYSCHEM 3 (2002) 98.
[29] B. Hartke, A. Charvat, M. Reich, B. Abel, J. Chem. Phys. 116 (2002) 3588.
[30] C. Lee, C. Sosa, M. Planas, J.J. Novoa, J. Chem. Phys. 104 (1996) 7081.
[31] J.R. Vacher, M. Jorda, E.L. Luc, M. Fitaire, Int. J. Mass Spectrom. Ion Processes 114 (1992) 149.
[32] A. Wakisaka, H. Kobara, J. Mol. Liquids 88 (2000) 121.
[33] M. Marsili, Y.-C. Zhang, Phys. Rev. Lett. 77 (1996) 3577.
[34] F. Kun, H.J. Herrmann, Phys. Rev. E 59 (1999) 2623.
[35] C. Mair, T. Fiegele, R. Wörgötter, J.H. Futrell, T.D. Märk, Int. J. Mass Spectrom. 177 (1998) 105.
[36] C. Mair, Z. Hermann, J. Fedor, M. Lezius, T.D. Märk, J. Chem. Phys. 118 (2003) 1479.
[37] P.A. Thiel, T.E. Madey, Surf. Sci. Rep. 7 (1987) 211.
[38] H.B. Bonzel, G. Pirug, C. Ritke, Langmuir 7 (1991) 3006.
[39] F. Mercuri, C.J. Mundy, M. Parrinello, J. Phys. Chem. A 105 (2001) 8423.
[40] V. Grill, J. Shen, C. Evans, R.G. Cooks, Rev. Sci. Instrum. 72 (2001) 3149.
[41] A. Tomsic, H. Schröder, K.L. Kompa, C.R. Gebhardt, J. Chem. Phys. 119 (2003) 6314.
[42] D.N. Shin, J.W. Wijnen, J.B.F.N. Engberts, A. Wakisaka, J. Chem. Phys. B 105 (2001) 6759.
[43] G. Raina, G.U. Kulkarni, Chem. Phys. Lett. 337 (2001) 269.
[44] A.S. Clarke, R. Kapral, G.N. Patey, J. Chem. Phys. 101 (1994) 2432.
[45] I. Ohmine, H. Tanaka, Chem. Rev. 93 (1993) 2545.
[46] M. Eigen, L. De Maeyer, Z. Elektrochem. 59 (1955) 986.
[47] D.J. Anick, J. Phys. Chem. A 107 (2003) 1348.
[48] J.-L. Kuo, C.V. Ciobanu, L. Ojamäe, I. Shavitt, S.J. Singer, J. Chem. Phys. 118 (2003) 3583.
[49] A.A. Vostrikov, D.Y. Dubov, M.R. Predtechenskiy, Chem. Phys. Lett. 139 (1987) 124.
[50] A.A. Vostrikov, A.M. Zadorozhny, D.Y. Dubov, G. Witt, I.V. Kazakova, O.A. Bragin, V.G. Kazakov, V.N. Kikhtenko, A.A. Tyutin, Z. Phys. D 40 (1997) 542.
[51] P.U. Andersson, J.B.C. Pettersson, 1997. Z. Phys. D, 41, 57.
[52] Q. Zhong, A.W. Castleman Jr., Chem. Rev. 100 (2000) 4039.
[53] C. R. Gebhardt, G. Tussiwand, H. Schröder, K. L. Kompa, in: Proceedings of the Eighth International Workshop on Rocket Propulsion: Present and Future, Pozzuoli, Italy, 2002, p. 46.